A Generic Approach to Modeling Vehicle Pitch Dynamics on a Vehicle Test Bench

CLEMENS KURZ (Graduate Student Member, IEEE), **LEON STANGENBERG, AND FRANK GAUTERIN**

Institute of Vehicle System Technology - Division of Vehicle Technology, Karlsruhe Institute of Technology (KIT), 76131 Karlsruhe, Germany

CORRESPONDING AUTHOR: CLEMENS KURZ (e-mail: clemens.kurz@kit.edu).

ABSTRACT The complexity of ADAS (Advanced Driving Assistance Systems) and AD (Autonomous Driving) functions increased in the last years. As the effort required for conventional test methods has grown significantly, new test procedures on vehicle test benches have been developed. This article deals with Vehicle in the Loop testing on vehicle test benches for ADAS and AD functions. The focus is set on the vehicle body movements caused by the vehicle on the test bench. For this purpose, the different pitch motions for road and test bench are derived using a vehicle dynamics model. On this basis, a novel model approach is developed, which uses the Lagrange's II. equation to determine the pitch motion of the vehicle on the test bench. The validity of the new model approach is confirmed by measurements and creates a generic basis to consider the influence of the vehicle's pitch motion while testing ADAS and AD functions on a vehicle test bench.

INDEX TERMS ADAS Testing, Road Vehicle Testing, Road Vehicle Dynamics, Vehicle Test Bench.

I. INTRODUCTION

In recent years, the development of Advanced Driving Assistance Systems (ADAS) and Autonomous Driving (AD) has progressed and reached a new level of complexity. For such complex development projects, it is necessary to use a systems engineering process. The commonly used V-Model, see [1], [2], [3], defines for every layer in the development process a corresponding procedure to test the defined functions. This ensures cross-domain communication during the development process and improves the development process. On the left side of the V-Model, the requirements for the functions are defined. The system description proceeds from a general requirement definition in the system layer to a specific requirement definition in the component layer. The right side of the V-Model defines the tests for every layer and their defined requirements. For testing ADAS and AD functions, a Vehicle in the Loop (ViL) test procedure is needed and can be classified in the system layer of the V-Model. When using a conventional testing procedure, the validation of ADAS and AD functions requires several million kilometers on test tracks and on public roads due to the statistical calculations of the safety requirement of the driving function, see [4]. This is caused by the non-repeatable environment conditions as weather and daytime [5]. New validation methods are developed for the use of vehicle test benches to increase testing and validation of the ADAS and AD functions. In test benches, the environment condition is repeatable and controllable. The Vehicle under Test (VuT) is tested as an entire system which includes the sensors, the automated driving functions, and the powertrain of the vehicle. But therefore, it is necessary to simulate or stimulate the environmental sensors like camera, radar, lidar, and ultrasonic sensors. Publication [6] demonstrated a camera stimulation on the test bench with screens, [7], [8], and [9] showed different methods for Over The Air (OTA) radar target simulation at vehicle test benches. OTA target simulation has the advantage to validate the overall ADAS and AD system, including the sensors (sense), data processing and planning (plan) and the vehicle with its powertrain (act). Especially OTA stimulation on a test bench represents a new challenge which is presented in this publication and relevant to every perception sensor.

A. MOTIVATION

The challenge in testing ADAS and AD functions on test benches is to guarantee a precise and valid environmental sensor stimulation with the external influencing factors being
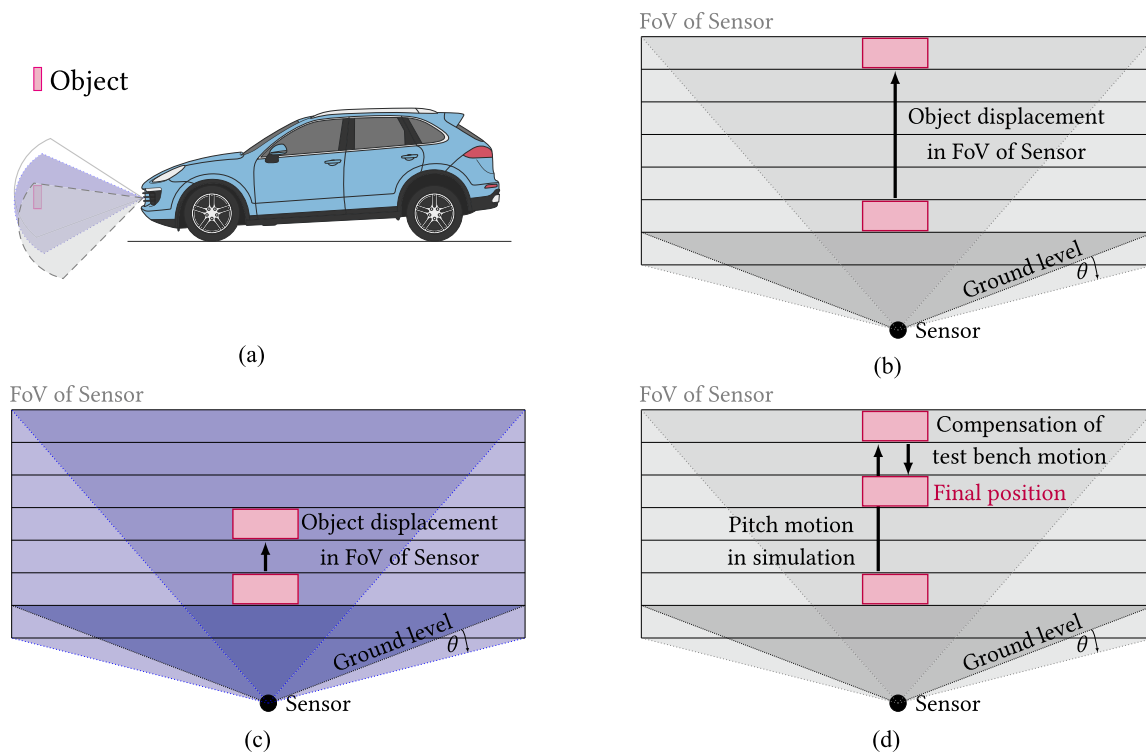
FIGURE 1. Object displacement in the FoV of the tracked object caused by a braking maneuver.; (a) Comparison of movement of the FoV on the road and on the test bench; (b) shows the object displacement in the FoV of the sensor during pitch motion on the street; (c) shows the object displacement in the FoV of the vehicle on the test bench; (d) shows how the body movements have to be considered to obtain a correct object simulation.

considered. In this context, the vehicle body movements on the vehicle test bench have to be modeled properly. If the vehicle body movement on the test bench is not considered correctly in the sensor simulation, this results in an incorrect validation of the ADAS and AD function. Two different vehicle body movements have to be taken into account. One is the vehicle body movement in the vehicle simulation of the test bench which is similar to a vehicle driving on the road. The other is the vehicle body movement that actually occurs on the test bench. Fig. 1 shows how the tracked object moves relative to the sensor's Field of View (FoV). Fig. 1 a) gives an overview of the different FoVs compared to the FoV in continuous driving. b) demonstrates how the object moves in the FoV when the vehicle brakes. The object in front of the car is still at the same position, but moves upwards in the sensor's FoV due to the pitch motion. This behavior reflects the displacement on the road which is simultaneous to the scenario simulation of the test bench. c) shows that the displacement on the test bench is different. Since the simulation assumes a non-moving vehicle, the vehicle's own motion must be compensated on the test bench, see d). Otherwise, the displacement would be added to the simulated displacement.

This article presents a novel approach to considering the vehicle body movement while testing ADAS and AD functions on vehicle test benches. The modeling of the vehicle body movement on a test bench as not yet been studied in detail.

B. STATE OF THE ART ANALYSIS

Many models for vehicle suspension and its dynamics are discussed in literature [10], [11]. A common model is the vehicle quarter model [12]. It is used for analyzing the vertical movement. The single-track model [13] is a plane dynamic model that does not consider vehicle body movements. The dual-track model is a more proper way to describe the vehicle body movements roll and pitch. However, this model is not suited for our application, because it has too many degrees of freedom. Thus, the model becomes too complex and many equations have to be solved unnecessarily. Mantaras et al. [14] used a vehicle dynamics model for a virtual test rig. This model is based on the tire road interaction of a vehicle on the real road. But the test bench in this article has no tire road interaction. Thus, this model is not suitable for this problem. Furthermore, there are several publications which have focused on the modeling of the vehicle body movements on the road [15], [16], [17], [18], [19], [20]. Similarly to [14], those publications also use the tire road interaction as basis of their model approaches. Additionally models with tire treadmill interaction exist. For this, [21] developed a model for vehicle body movement on a steerable roller dynamometer with multibody simulation.

A highly interesting approach is the modeling of the vehicle body movements with the II. Lagrange-Equation. For NVH (Noise Vibration Harshness) issues, the analysis of road vehicle body movements with Lagrange is standard. Jazar [22]
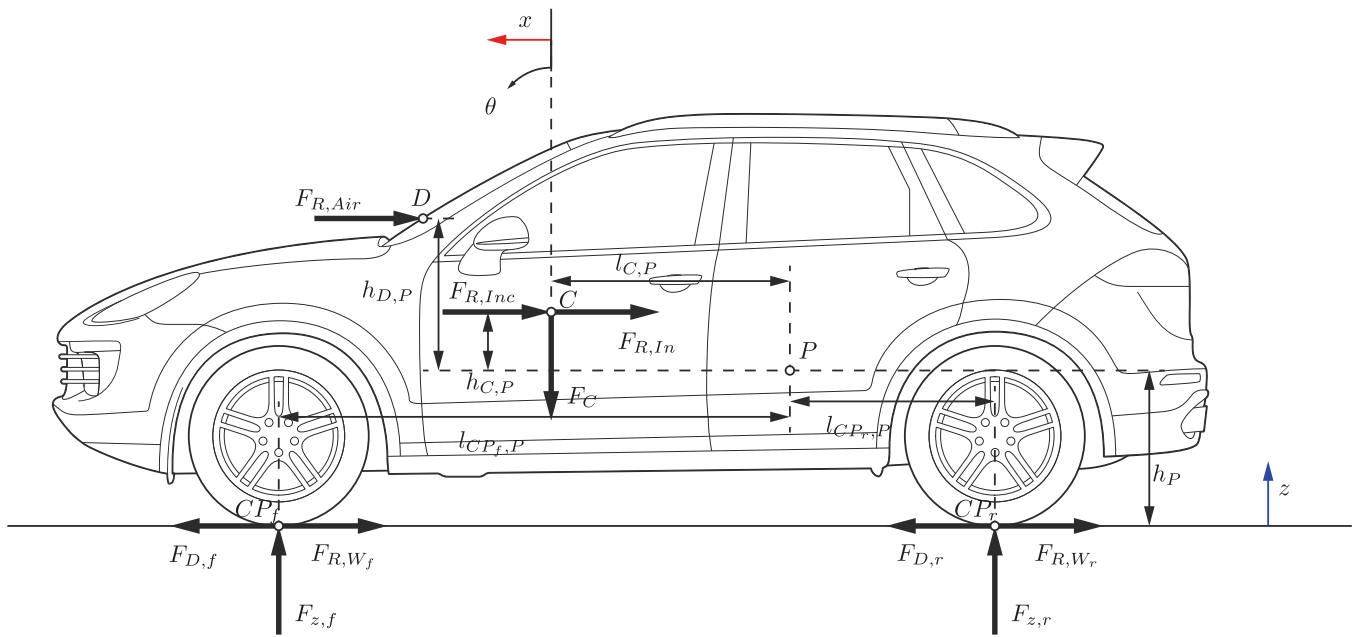
FIGURE 2. External forces on a vehicle on the road.

calls this kind of model a bicycle model for vehicles [22, p. 843].

In summary, many different model approaches already exist for vehicle body movements under real road conditions. But most of them are difficult to transfer to the test bench vehicle body movements. The Lagrangian modeling approach is the most promising one and can be adapted and improved in this article. The focus of this research is on a generic, adaptable model. The specific aim is to develop a model which uses the information a test bench operator already receives from the test bench. No further improvements, such as additional sensors, will be required to use the model while testing the ADAS and AD functions.

II. DIFFERENCES OF THE EXTERNAL FORCES ON THE REAL ROAD COMPARED TO VEHICLE TEST BENCH

For modeling the vehicle pitch motion on test benches, it is necessary to find out why the current approaches of vehicle body models for road conditions are not suitable. Therefore, a comparison of the external forces of the vehicle is needed to understand, that there are differences in the root cause of the vehicle body motions on the road and on the test bench.

A. VEHICLE ON THE REAL ROAD

The vehicle on the real road is subjected to a number of external forces. Those external forces include the result of the inner forces of constraint and anti-geometries in the suspension. Most of these forces are known as the driving resistance forces the vehicle has to overcome. The forces on a vehicle can be cut free for any slope and be marked in Fig. 2:

- Weight force F_C in the center of mass C

- Dynamic wheel load F_z in the respective tire contact point CP
- Tire resistance forces $F_{R,W}$ in the respective CP
- Inertia force $F_{R,In}$ in C
- Inclination force $F_{R,Inc}$ in C
- Aerodynamic force $F_{R,Air}$ in the center of pressure D
- Driving force F_D in the respective CP.

The lengths given here refer to the center of rotation for pitch motion P. The pitch angle is given as θ. The following derivation is based on the assumption that the road surface is level $\alpha = 0$.

PITCH MOTION ON THE ROAD

The pitch motion of the vehicle on the road depends on the inertia forces, the acceleration or brake forces, the position of the pitch center, and the anti-geometries against the pitch motion. For simplification, the instant center of rotation for pitch motion P does not move with the pitch angle. For the external forces in Fig. 2 the following generally valid relationships are known.

$$F_C = m \cdot g \tag{1}$$

$$F_{R,In} = m \cdot \ddot{x} \tag{2}$$

$$F_{R,Air} = \frac{1}{2} \cdot \rho \cdot c_w \cdot A \cdot v_{rel}^2 \tag{3}$$

$$F_{R,Inc} = F_C \cdot \sin(\alpha) \tag{4}$$

$$F_{R,W} = F_{RR} + F_{R\gamma} + F_{RFl} \tag{5}$$

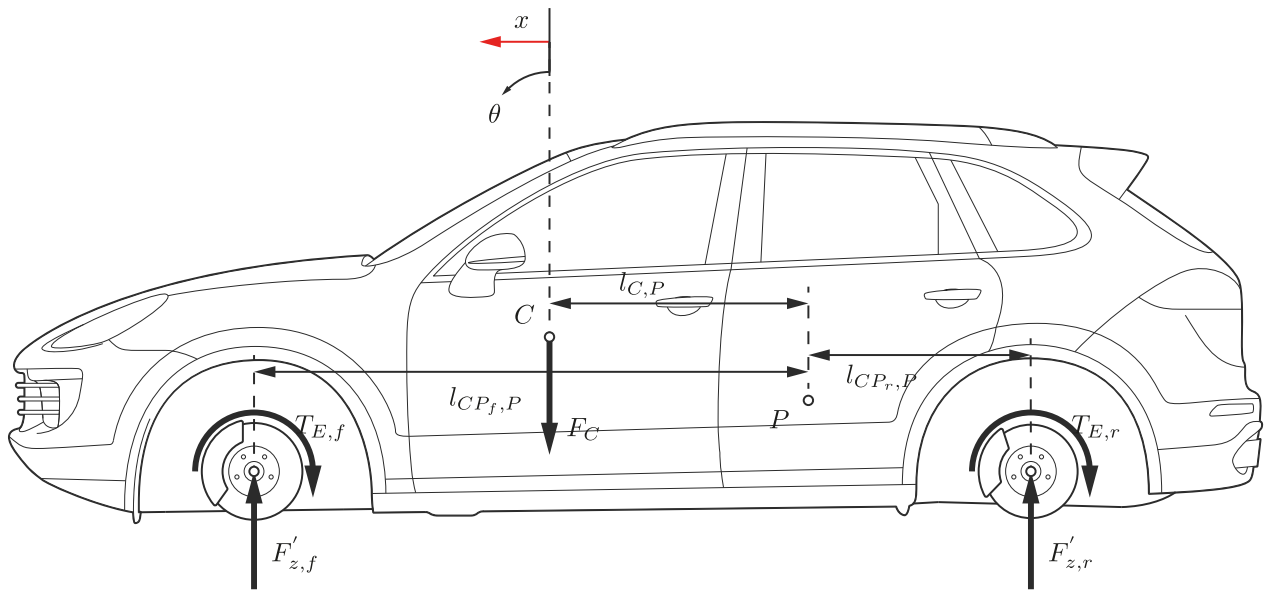$$F_R = F_{R,In} + F_{R,W} + F_{R,Air} + F_{R,Inc} = \sum_{(i)} F_i \tag{6}$$

FIGURE 3. External forces on a vehicle on a test bench.

F_{RR} is the rolling resistance force, $F_{R\gamma}$ is the side-slip resistance force, and F_{RFl} is the flood resistance force, which occurs during rain. These resistance force components are not explained in detail. The reader is referred to [23].

For simplification, the resistance forces and their lever arm from their contact point to the pitch center are summarized in total torque from resistances $T_{R,i}$

$$T_{R,i} = \sum_{(i)} F_i \cdot h_i. \tag{7}$$

The sum of all torques in P using (7) is

$$\sum T^{(P)} = T_{Ri} - F_D \cdot h_P + F_C \cdot l_{C,P} - F_{z,f} \cdot l_{CP_f,P}$$
$$+ F_{z,r} \cdot l_{CP_r,P} - \ddot{\theta} \cdot J_P = 0. \tag{8}$$

This (8) will be needed later for the comparison between road and test bench pitch motion.

B. VEHICLE ON THE TEST BENCH

The vehicle test bench presented in this publication is a powertrain test bench. The special feature of this kind of test bench is that the tires have to be dismounted. For a more detailed description of the test bench, see Section IV. In contrast to the real road, the following forces and torques occur on the free-cut vehicle mounted on the test bench, see Fig. 3:

- Weight force F_C in the center of mass C
- Dynamic wheel load F_z' in the respective wheel contact point CP
- Torque of the electric load machines T_E in each wheel hub

The torque provided by the load machines is based on the assumption that the vehicle on the test bench should face the same resistance forces as a vehicle on the road. This is

necessary to guarantee a realistic transferability from road to test bench. The resistance forces on the test bench are calculated in simulations. These calculations handle the car as if it was driving on the road to determine a realistic resistance force. The forces are acting in the contact point between the tire slack and the road surface. On powertrain test benches, however, the resistance forces can only be initiated by torque in the wheel hubs of the vehicle under test (VuT) and not by forces. This results in a further calculation of the resistance forces with the dynamic tire radius r_{dyn}:

$$T_e = F_R \cdot r_{dyn}. \tag{9}$$

Due to the lacking longitudinal movement of the vehicle, there is no moment of inertia acting in the center of mass. To achieve a realistic movement behavior, it is necessary to simulate the moment of inertia on the test bench. This has to be added to the calculation of the torque for the electric load machines.

PITCH MOTION ON THE TEST BENCH

The pitch motion of the vehicle on the test bench can be derived from the sum of all torques in P.

$$\sum T^{(P)} = T_{E,f} + T_{E,r} + F_C \cdot l_{C,P} - F_{z,f}' \cdot l_{CP_f,P}$$
$$+ F_{z,r}' \cdot l_{CP_r,P} - \ddot{\theta} \cdot J_P = 0 \tag{10}$$

The difference of both pitch torque equations becomes obvious when both equations, (8) and (10), are equated and simplified. The result, Theorem 1, shows that the pitch motion of a vehicle on the road has a different root cause than a vehicle on a test bench.

Theorem 1: $T_{R,i} - F_D \cdot h_P \neq T_{e,f} + T_{e,r}$
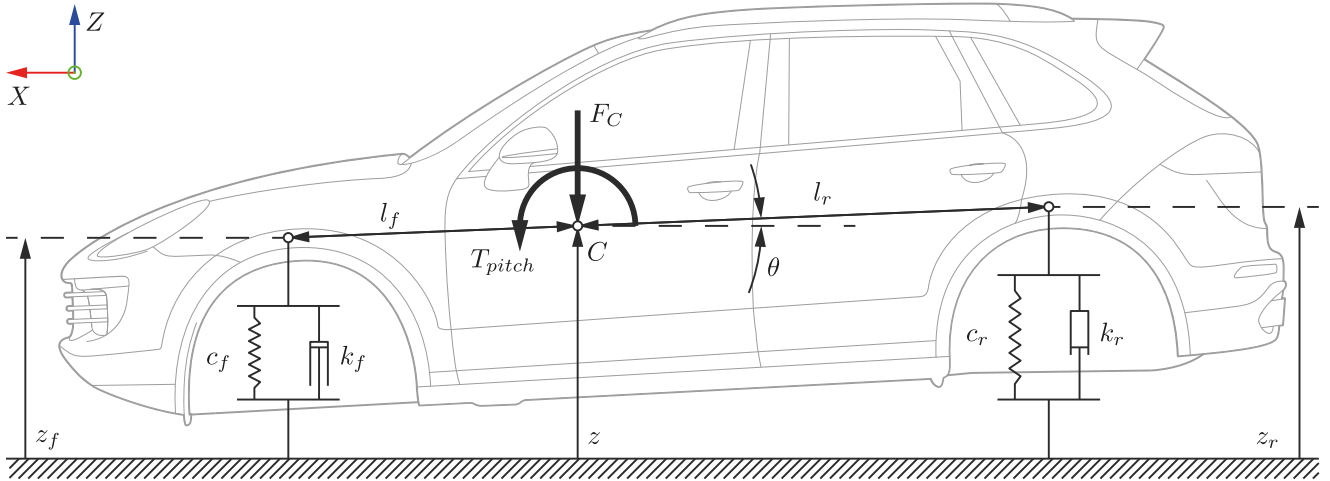
FIGURE 4. Motion model for describing the pitch motion on a test bench.

This means that the description of pitch motion on the road is not equal to that on the test bench and cannot be transferred. Considering the testing of ADAS and AD functions on the test bench, the result is that a model for the vehicle pitch motion is needed. The challenge is that the model should be used as a generic application with a minimum of inner vehicle parameters. The quantities $l_{C,P}$, $l_{CP_f,P}$ and $l_{CP_r,P}$ in (10) are too vehicle-specific and not freely accessible. Moreover, the measurement of the dynamic wheel load is difficult to realize on this test bench. That is why this model approach cannot be used and another approach is needed to solve this problem.

III. MODELING OF PITCH MOTION ON A VEHICLE TEST BENCH

The movement model has to be described with equations of motion. There are various options to set up the vehicle's equations of motion: The description of d'Alembert or the Lagrange's equations of motion. The advantage of the Lagrange's description is the fact that it is not necessary to determine the forces of constraint and torques for the model. The independent degrees of freedom in the system can be described in the form of generalized coordinates. For each generalized coordinate one equation of motion is required to solve the motion problem of the system. The Lagrange's equation of motion is chosen here.

As this model should solve the pitch motion, it is only necessary to consider one half of the vehicle. The model is based on the vocabulary of further publications of Jazar, see [22], [24].

The shown vehicle model demonstrates a car mounted on a power train test bench, Fig. 4. The suspension is modeled by a spring and a damper on each wheel. The weight force F_C and the pitch torque T_{pitch} act in the center of mass C. The pitch torque is the sum of all electric load machine torques which represent the driving resistance forces. The distance from the center of mass to the front wheel is described as l_f, l_r is the distance to the rear wheel.

The vehicle model has two degrees of freedom. They are described by two generalized coordinates q_1 and q_2

$$q_1 = z \tag{11}$$

$$q_2 = \theta. \tag{12}$$

q_1 describes the translation degree of freedom of the vehicle in the direction of the z-axis. q_2 describes the rotational degree of freedom around the y-axis of the vehicle.

There are also two auxiliary variables z_f for the motion of the car front and z_r for the motion of the rear part of the vehicle. Both variables can be determined as a function of the generalized coordinates:

$$z_f = z - l_f \sin(\theta) \tag{13}$$

$$z_r = z + l_r \sin(\theta). \tag{14}$$

The general Lagrangian equation is determined as

$$\frac{\mathrm{d}}{\mathrm{d}t} \frac{\partial L}{\partial \dot{q}_i} - \frac{\partial L}{\partial q_i} = Q_i. \tag{15}$$

The kinetic potential of the vehicle L will be determined with Lagrange's II. equation It is the result of the difference of the kinetic energy T and the potential energy V of all potential forces in the system (e.g., force of weight, spring force, ...).

$$L = T - V \tag{16}$$

$$T = \frac{1}{2}m\dot{z}^2 + \frac{1}{2}J_s\dot{\theta}^2 \tag{17}$$

$$V = \frac{1}{2}c_f(h - z_f)^2 + \frac{1}{2}c_r(h - z_r)^2 + mg(z - h) \tag{18}$$

$$L = \frac{1}{2}m\dot{z}^2 + \frac{1}{2}J_s\dot{\theta}^2 - \frac{1}{2}c_f(h - z_f)^2$$
$$- \frac{1}{2}c_r(h - z_r)^2 - mg(z - h) \tag{19}$$

Furthermore, the virtual work δW needs to be determined to obtain the generalized forces Q_1 and Q_2. With the help of
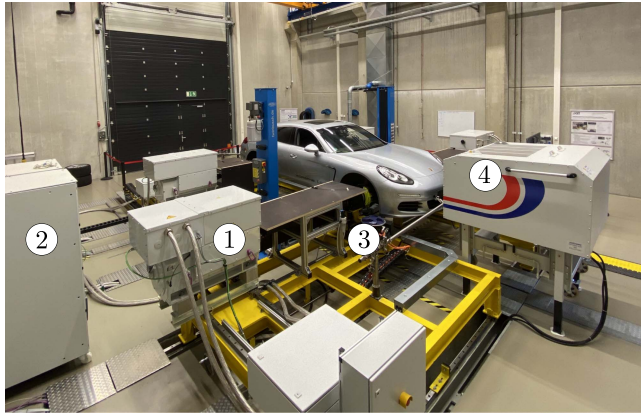
FIGURE 5. Vehicle-in-the-loop test bench at KIT-FAST.

TABLE 1 Technical Data of the Test Bench

Description	Data
Nominal wheel load power	209 kW
Max. wheel load torque at nom. speed (800 min^{-1})	2500 Nm
Max. wheel speed	2000 min^{-1} $\approx$ 260 km/h
Max. self-aligning torque at the front wheels	1000 Nm
Max. steering angle at the front wheels	$\pm 18°$
Max. air fan wind speed	135 km/h
Max. vehicle weight	12 000 kg
Max. wheel load	3000 kg
Wheelbase	$1.8 - 4.9$ m
Track width	$1.2 - 3.9$ m

the generalized fores, the equations of motion can finally be formulated.

The approach for the virtual work δW in a plane and non-vector case with an explicit extension of torques (see 5.9 in [25, p. 220]) is defined as:

$$\delta W = \sum_{j=1}^{n} \mathbf{F}_j \cdot \delta \mathbf{r}_j + \sum_{k=1}^{m} M_k \delta \phi_k \overset{!}{=} \sum_{i=1}^{f} Q_i \delta q_i \quad (20)$$

$\mathbf{F}_j$ are the potentialless forces and M_k are the potentialless torques which are not considered in V. In the explicit model (20) the virtual work is:

$$\delta W = -k_f \dot{z}_f \delta z_f - k_r \dot{z}_r \delta z_r + M_{pitch} \delta \theta \quad (21)$$

The time derivations of $\dot{z}_f$, $\dot{z}_r$, and the virtual displacements δz_f and δz_r need to be defined in the generalized coordinates. For the time derivations

$$\dot{z}_f = \dot{z} - l_f \dot{\theta} \cos(\theta) \quad (22)$$

$$\dot{z}_r = \dot{z} + l_r \dot{\theta} \cos(\theta) \quad (23)$$

result. The virtual displacements δz_f and δz_r can be calculated with the help of the general equation for virtual displacements $\delta \mathbf{r}_j$ (see Eq. 5.6a in [25, p. 220])

$$\delta \mathbf{r}_j = \sum_{(i)} \frac{\partial \mathbf{r}_j}{\partial q_i} \delta q_i. \quad (24)$$

The virtual displacement of the height of the front axle δz_f is defined as:

$$\delta z_f = \frac{\partial z_f}{\partial q_1} \delta q_1 + \frac{\partial z_f}{\partial q_2} \delta q_2 = \frac{\partial z_f}{\partial z} \delta z + \frac{\partial z_f}{\partial \theta} \delta \theta$$

$$= \delta z - l_f \cos(\theta) \delta \theta. \quad (25)$$

The similar calculation of (24) for δz_r results as:

$$\delta z_r = \delta z + l_r \cos(\theta) \delta \theta. \quad (26)$$

Inserting (22), (23), (25), and (26) into (21) gives the final result for the virtual work δW:

$$\delta W = M_{pitch} \delta \theta - k_f (\dot{z} - l_f \dot{\theta} \cos(\theta))(\delta z - l_f \cos(\theta) \delta \theta)$$
$$- k_r (\dot{z} + l_r \dot{\theta} \cos(\theta))(\delta z + l_r \cos(\theta) \delta \theta)$$

$$\overset{!}{=} Q_1 \delta z + Q_2 \delta \theta. \quad (27)$$

A comparison of coefficients in (27) for the virtual displacements δz and $\delta \theta$ provides the equation for the generalized force Q_1:

$$Q_1 = -k_f (\dot{z} - l_f \dot{\theta} \cos(\theta)) - k_r (\dot{z} + l_r \dot{\theta} \cos(\theta)) \quad . \quad (28)$$

For Q_2, it holds:

$$Q_2 = M_{pitch} + k_f l_f \cos(\theta)(\dot{z} - l_f \dot{\theta} \cos(\theta))$$
$$- k_r l_r \cos(\theta)(\dot{z} + l_r \dot{\theta} \cos(\theta)). \quad (29)$$

With the kinematic potential L and the generalized forces Q_1 and Q_2 it is possible to calculate the Lagrangian (15) to describe the motion of the vehicle. This equation is solved for $i = 1$ at first and afterwards for $i = 2$. Inserting of $q_1 = z$ and L from (19) and solving the differential equation result in

$$\frac{d}{dt} \frac{\partial L}{\partial \dot{z}} = m \ddot{z} \quad (30)$$

$$\frac{\partial L}{\partial z} = -mg + c_f (h - z + l_f \sin(\theta))$$
$$+ c_r (h - z - l_r \sin(\theta)). \quad (31)$$

To obtain the first equation of motion, (28), (30), and (31) are equated.

$$Q_1 \overset{!}{=} m \ddot{z} + mg - c_f (h - z + l_f \sin(\theta))$$
$$- c_r (h - z - l_r \sin(\theta)). \quad (32)$$

After a few transformations, the result of (32) is

$$m \ddot{z} + (k_f + k_r) \dot{z} + (c_f + c_r) z + (k_r l_r - k_f l_f) \dot{\theta} \cos(\theta)$$
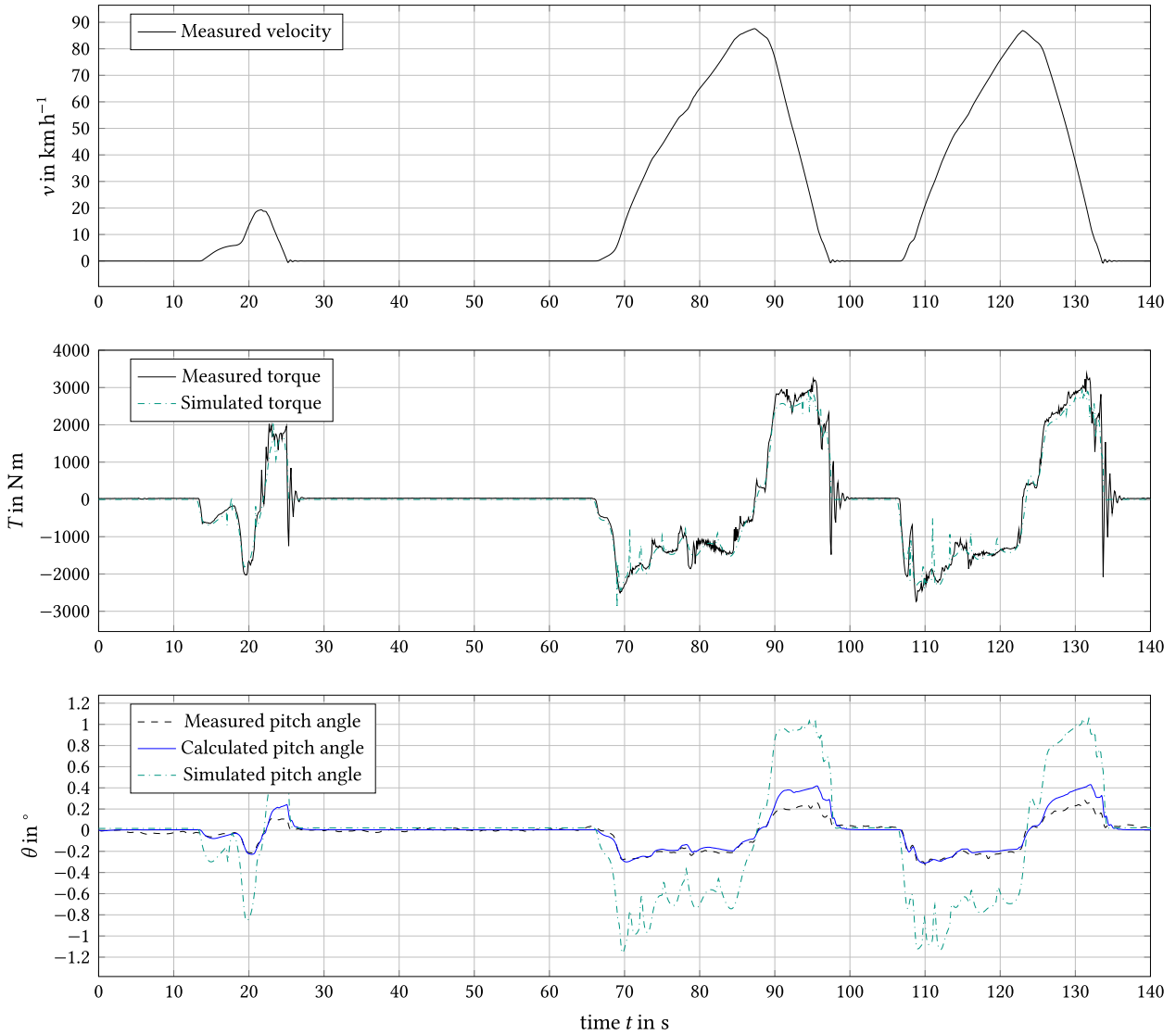$$+ (c_r l_r - c_f l_f) \sin(\theta) = -mg + (c_f + c_r) h. \quad (33)$$

FIGURE 6. Measurement of the pitch angle of two acceleration runs with normal resistance forces on the test bench.

For the second equation of motion, $q_2 = \theta$ and the following differential equation has to be solved.

$$\frac{\mathrm{d}}{\mathrm{d}t}\frac{\partial L}{\partial \dot{\theta}} = J_s \ddot{\theta} \tag{34}$$

$$\frac{\partial L}{\partial \theta} = -c_f(h - z + l_f \sin(\theta))l_f \cos(\theta)$$
$$+ c_r(h - z - l_r \sin(\theta))l_r \cos(\theta) \tag{35}$$

Equations (29), (34), and (35) are equated and transformed, similar to the determination of (33).

$$M_{pitch} = J_s \ddot{\theta} + (k_f l_f^2 + k_r l_r^2)\dot{\theta}\cos^2(\theta)$$
$$+ (c_f l_f^2 + c_r l_r^2)\sin(\theta)\cos(\theta)$$
$$+ (k_r l_r - k_f l_f)\dot{z}\cos(\theta) + (c_r l_r - c_f l_f)z\cos(\theta)$$
$$+ (c_f l_f - c_r l_r)h\cos(\theta) \tag{36}$$

With the two equations of motion, (33) and (36), it is possible to describe the pitch motion of a vehicle on a test bench. The only variable input parameter of this model approach is the torque of the test bench's load machines that is already measured on every vehicle test bench. Thus, this model approach is independent of a specific test bench and can be used generically for vehicle test benches. But it only works with test benches where the vehicle does not have to be tethered which is the case with roller dynamometers. Tethering results in additional forces on the system and will reduce the pitch motion of the vehicle. So, this model is not adaptable to roller dynamometers.

IV. VALIDATION OF PITCH MODEL
A. VEHICLE TEST BENCH
The vehicle-in-the-loop test bench at the KIT Institute of Vehicle System Technology is a powertrain test bench, see
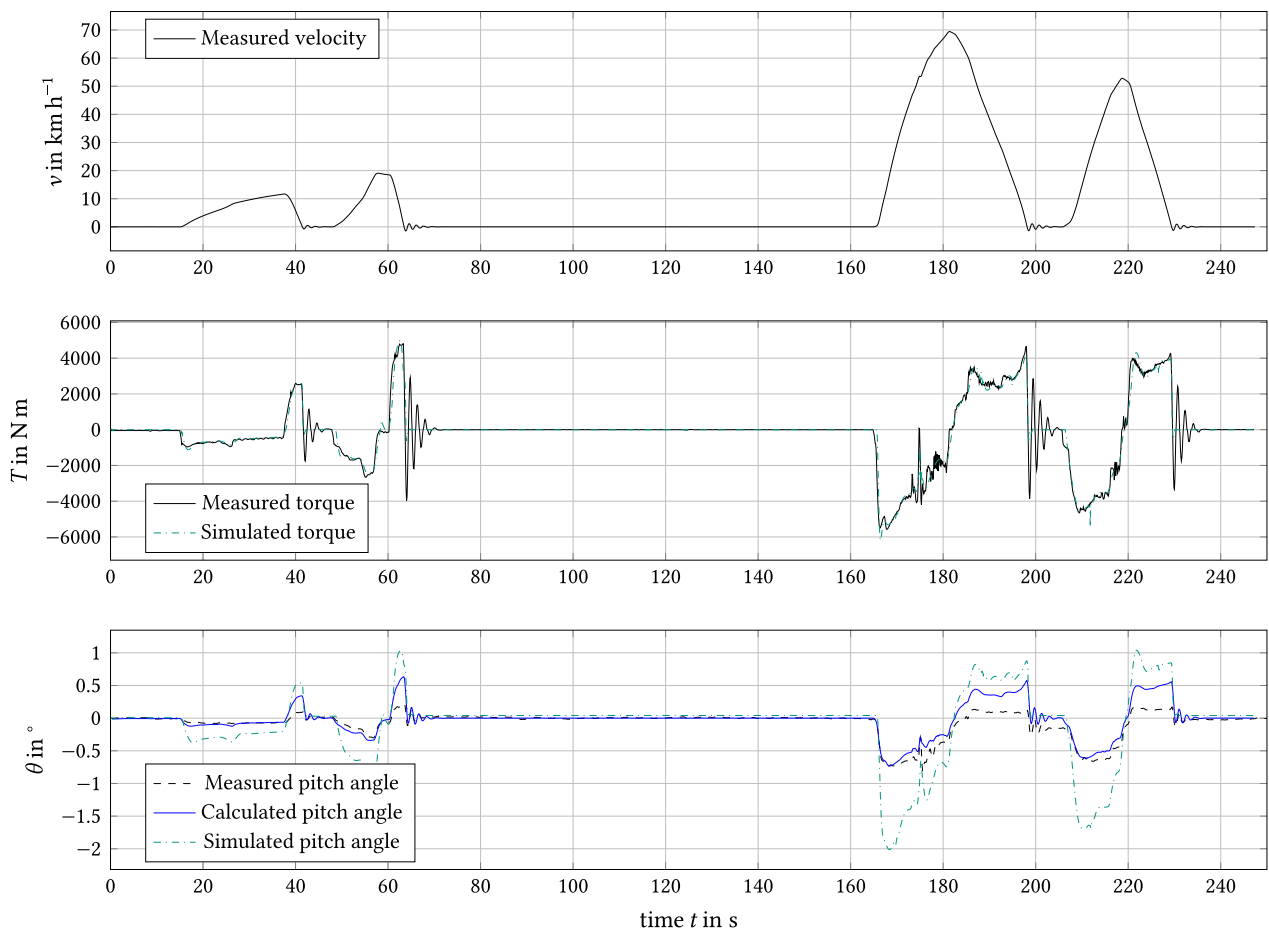
FIGURE 7. Measurement of the pitch angle of two acceleration runs with high resistance forces on the test bench.

Fig. 5. It can be used for vehicle research in longitudinal and lateral dynamic driving situations. For this kind of test bench, each vehicle tire has to be dismounted, and the wheel hub is connected to an electric load machine (1). The electric load machines are controlled by highly dynamic frequency converters (2). The connection between wheel hub and load machine is achieved by a constant velocity joint shaft. With this special shaft, it is possible to steer and drive the front axle simultaneously for dynamic longitudinal and lateral scenarios. A realistic steering behavior is realized by two synchronous engines (3) which deliver a self-aligning torque for each wheel individually. The vehicle on the test bench is cooled by an air fan (4) and ensures an air flow for the heat dissipation of different vehicle parts, for example, powertrain and brake disks. For a more detailed description of the test bench, see [27]. The main technical data of the test bench are presented in Table 1.

B. VALIDATION DATA

The validation data of the pitch motion is measured by an acceleration sensor. To avoid measurement falsification, the data has to be filtered with a low-pass filter. The cut-off frequency of the filter is chosen to be 10 Hz because vehicle body movements generally occur at lower frequencies, see [10,

p. 139]. The measured validation data of the pitch motion and the test bench data, e.g. velocity and torque, are recorded by two different measuring systems. This results in a temporal shift of the measured signals. The temporal shift is solved by using the cross correlation of both signals.

The scenarios for both measurements are acceleration experiments. The first measurement is run with normal resistance forces and the second measurement is driven with higher resistance forces to get an overrated pitch motion. In addition, vehicle simulations are performed with the acceleration and resistance forces. This enables direct comparison of the simulated vehicle and its object displacement in the FoV with the vehicle on the bench, as described in Fig. 1. The simulations are performed with IPG CarMaker.

In the following part, two validation measurements are shown and discussed. The measurement has to be considered under given internal parameters for mass inertia, damping and spring coefficients.

VALIDATION MEASUREMENTS

In the first measurement, see Fig. 6, the vehicle is accelerated with $2.5 \, \text{m/s}^2$ to $90 \, \text{km/h}$. After reaching the maximum speed, the vehicle is decelerated with $-3.5 \, \text{m/s}^2$ to standstill.

The torque resulting from the driving resistance calculation varies between $-2200\,\text{Nm}$ for acceleration and $3400\,\text{Nm}$ for braking. In the simulation the gear shift can be identified by small jumps in the torque curve. The pitch angle that occurs as a result of the acceleration phases is around $\theta_{meas,\min} = -0.35°$. The resulting pitch angle for the braking phase is $\theta_{meas,\max} = 0.28°$. The calculated pitch angle based on the model of the vehicle body movement is close to the measured data with $\theta_{calc,\min} = -0.37°$ in the acceleration phase. The vehicle in the simulation has higher pitch angles around $\theta_{sim,\min} = -1.1°$ for acceleration and around $\theta_{sim,\max} = 1°$ in the braking phase. Also the gear shifts can be recognized in the pitch curve. A bigger error between the measured and calculated pitch angle is found in the braking phase of the vehicle. Here, the pitch angle in the model is calculated as $\theta_{calc,\max} = 0.41°$.

For the second measurement, see Fig. 7, the driving resistance forces are parameterized higher than usual. The result is that the acting torques and the occurring pitch motion are much higher for a better validation of the model. In comparison to the first measurement, the maximum velocity is reduced to $v_{\max} = 69\,\text{km/h}$. The torque increases to $-5574\,\text{Nm}$ during the acceleration phase. This results in a pitch motion of $\theta_{meas} = \theta_{calc} = -0.73°$ at $t = 168\,\text{s}$. That confirms the validity of the model in extension movements. The second measurements prove that the model is not perfectly valid for compression movements (braking) of the vehicle. The deceleration creates a pitch motion of $\theta_{meas} = 0.13°$, whereas the model calculates a pitch angle of $\theta_{calc} = 0.44°$ at $t = 192\,\text{s}$. The simulation of the real vehicle shows a significantly higher pitch motion of the vehicle with almost the same torque curve. The gear shift also has an influence on the acting torque and the resulting pitch motion. The simulated vehicle reaches $\theta_{sim,\min} = -2.01°$, i.e. a pitch angle that exceeds the measured and calculated values by a factor of about 3.

C. DISCUSSION

The measurement results show that the pitch motion of a simulated real vehicle is up to three times higher than the pitch angle of the vehicle on the test bench. It is shown that fits in the modeling of the extension good. However, modeling braking is a problem due to an inaccuracy of the damper modeling. A realistic shock absorber (damper) has two different damper coefficients for compression and rebound. The presented pitch model has only one damper coefficient for both. The damper coefficient was fitted for rebound. This results in the mentioned inaccuracy during braking. To solve this issue, damper modeling needs to be extended. Therefore, the damper has to become a speed-dependent coefficient and is dependent on the generalized coordinate $\dot{z}$ of the pitch model.

V. CONCLUSION

This publication investigates a model for the pitch motion of a vehicle mounted on a powertrain test bench, which is validated by measurements on the test bench. The validation shows that the vehicle model is accurate for an acceleration

process and the vehicle's deflection. For a deceleration and the resulting compression of the suspension the model differs from reality. A possible explanation for this is the simple damper model which is chosen with a linear damping ratio. But the real damper is usually built with two different damping ratios for compression and extension and has energy dissipation.

Hence, further investigations for a more precise vehicle model are needed. The individual chassis parts have to be modeled more precisely:

- model for anti-geometries
- advanced damper model with different rebound and compression damping ratios

Furthermore, this model approach can be adapted for modeling the vehicle roll motion on a vehicle test bench.

Nevertheless, this model allows to determine the vehicle's pitch motion only on the basis of the measured driving resistance torque and can be considered in the sensor target simulation of the test bench. This ensures a precise validation of the ADAS and AD function on vehicle test benches.

REFERENCES

[1] *Entwicklungsmethodik Für Mechatronische Systeme - Design Methodology for Mechatronic Systems, 2206*. Berlin, Germany: Verein Deutscher Ingenieure, Nov. 2021.

[2] I. Graessler, J. Hentze, and T. Bruckmann, "V-Models for interdisciplinary systems engineering," in *Proc. 15th Int. Des. Conf.*, 2018, pp. 747–756.

[3] H. Winner, S. Hakuli, F. Lotz, and C. Singer, Eds., *Handbook of Driver Assistance Systems: Basic Information, Components and Systems for Active Safety and Comfort*. Cham, Switzerland: Springer, 2016, doi: 10.1007/978-3-319-12352-3.

[4] N. Kalra and S. Paddock, *Driving to Safety: How Many Miles of Driving Would It Take to Demonstrate Autonomous Vehicle Reliability?:* Santa Monica, CA, USA: RAND Corporation, 2016.

[5] P. Koopman and M. Wagner, "Challenges in autonomous vehicle testing and validation," *SAE Int. J. Trans. Saf.*, vol. 4, no. 1, pp. 15–24, 2016, doi: 10.4271/2016-01-0128.

[6] S. Solmaz, F. Holzinger, M. Mischinger, M. Rudigier, and J. Reckenzaun, "Novel hybrid-testing paradigms for automated vehicle and ADAS function development," in *EAI/Springer Innovations in Communication and Computing, Towards Connected and Autonomous Vehicle Highways*, U. Z. A. Hamid and F. Al-Turjman, Eds. Cham, Switzerland: Springer, 2021, pp. 193–228, doi: 10.1007/978-3-030-66042-0_8.

[7] S. B. J. Gowdu, M. E. Asghar, R. Stephan, M. A. Hein, J. Nagel, and F. Baumgartner, "System architecture for installed-performance testing of automotive radars over-the-air," in *Proc. IEEE MTT-S Int. Conf. Microw. Intell. Mobility*, 2018, pp. 1–4.

[8] A. Diewald et al., "Radar target simulation for vehicle-in-the-loop testing," *Vehicles*, vol. 3, no. 2, pp. 257–271, 2021, doi: 10.3390/vehicles3020016.

[9] A. Gruber et al., "Highly scalable radar target simulator for autonomous driving test beds," in *Proc. IEEE Eur. Radar Conf.*, 2017, pp. 147–150.

[10] S. Taheri, C. Sandu, B. L. Duprey, and T. D. Gillespie, Eds., *Fundamentals of Vehicle Dynamics*. Warrendale, PA, USA: SAE Int., 2021.

[11] D. Cao, X. Song, and M. Ahmadian, "Editors' perspectives: Road vehicle suspension design, dynamics, and control," *Veh. Syst. Dyn.*, vol. 49, no. 1/2, pp. 3–28, 2011, doi: 10.1080/00423114.2010.532223.

[12] H. Benaroya, *Mechanical Vibration*. Boca Raton, FL, United States: CRC Press, 2004. doi: 10.1201/9781420056143.

[13] S. Breuer and A. Rohrbach-Kerl, *Fahrzeugdynamik: Mechanik des bewegten Fahrzeugs*. Wiesbaden, Germany: Springer Vieweg, 2015, doi: 10.1007/978-3-658-09475-1.

[14] D. A. Mántaras and P. Luque, "Virtual test rig to improve the design and optimisation process of the vehicle steering and suspension systems," *Veh. Syst. Dyn.*, vol. 50, no. 10, pp. 1563–1584, 2012, doi: 10.1080/00423114.2012.680472.

[15] H. E. Tseng, L. Xu, and D. Hrovat, "Estimation of land vehicle roll and pitch angles," *Veh. Syst. Dyn.*, vol. 45, no. 5, pp. 433–443, 2007, doi: 10.1080/00423110601169713.

[16] Z. Guo, W. Wu, and S. Yuan, "Longitudinal-vertical dynamics of wheeled vehicle under off-road conditions," *Veh. Syst. Dyn.*, vol. 60, no. 2, pp. 470–490, 2022, doi: 10.1080/00423114.2020.1823003.

[17] J. S. Kang, J. K. Lee, and D. Bae, "A chassis-based kinematic formulation for flexible multi-body vehicle dynamics," *Mechanics Based Des. Struct. Mach.*, vol. 45, no. 1, pp. 12–24, 2017, doi: 10.1080/15397734.2015.1126693.

[18] J. Oh and S. B. Choi, "Vehicle roll and pitch angle estimation using a cost-effective six-dimensional inertial measurement unit," *Proc. Inst. Mech. Eng. Part D: J. Automobile Eng.*, vol. 227, no. 4, pp. 577–590, 2013, doi: 10.1177/0954407012459138.

[19] R. S. Sharp, "Influences of suspension kinematics on pitching dynamics of cars in longitudinal manoeuvring," *Veh. Syst. Dyn.*, vol. 33, no. sup1, pp. 23–36, 1999, doi: 10.1080/00423114.1999.12063067.

[20] G. Xu, N. Zhang, and H. M. Roser, "Roll and pitch independently tuned interconnected suspension: Modelling and dynamic analysis," *Veh. Syst. Dyn.*, vol. 53, no. 12, pp. 1830–1849, 2015, doi: 10.1080/00423114.2015.1103375.

[21] A. Ahlert, *Ein Modellbasiertes Regelungskonzept Für Einen Gesamtfahrzeug-Dynamikprüfstand*. Wiesbaden, Germany: Springer Fachmedien Wiesbaden GmbH, 2020. [Online]. Available: https://ebookcentral.proquest.com/lib/kxp/detail.action?docID=6177153

[22] R. N. Jazar, *Vehicle Dynamics: Theory and Application*, 3rd ed. Cham, Switzerland: Springer, 2017. ISBN 978-3-319-53441-1.

[23] M. Ersoy and S. Gies, *Fahrwerkhandbuch: Grundlagen - Fahrdynamik - Fahrverhalten- Komponenten - Elektronische Systeme - Fahrerassistenz - Autonomes Fahren- Perspektiven*. Wiesbaden, Germany: Springer, 2017. [Online]. Available: https://ebookcentral.proquest.com/lib/gbv/detail.action?docID=4884381

[24] R. N. Jazar, *Vehicle Dynamics: Theory and Application*, 2nd ed. New York, NY, USA: Springer, 2014.

[25] J. Mareczek, *Grundlagen Der Roboter-Manipulatoren – Band 1*. Berlin, Heidelberg, Germany: Springer, 2020.

[26] D. Ammon, *Modellbildung und Systementwicklung in der Fahrzeugdynamik*. Stuttgart, Germany: Teubner.

[27] P. Rautenberg, C. Kurz, M. Gießler, and F. Gauterin, "Driving robot for reproducible testing: A novel combination of pedal and steering robot on a steerable vehicle test bench," *Vehicles*, vol. 4, no. 3, pp. 727–743, Jul. 2022, doi: 10.3390/vehicles4030041.

CLEMENS KURZ (Graduate Student Member, IEEE) was born in Karlsruhe, Germany in 1994. He received the B.Eng. degree in mechanical engineering from the University of Applied Sciences Karlsruhe, Karlsruhe, Germany, in 2017 and the M.Sc. degrees in mechanical engineering from the University of Applied Sciences Mannheim, in 2019. He is currently working toward the Doctoral degree in mechanical engineering with the Institute of Vehicle System Technology (FAST) at Karlsruhe Institute of Technology (KIT), Karlsruhe. His research focuses on procedures for testing radar based ADAS functions on vehicle test benches.

LEON STANGENBERG was born in Hamburg, Germany, in 1997. He received the B.Sc. in mechanical engineering from Karlsruhe Institute of Technology (KIT), Karlsruhe, Germany in 2021. He is currently working toward the M.Sc. degree with KIT. His research interest include vehicle control, vehicle automation, and computer vision mainly for mobile working machine applications.

FRANK GAUTERIN received the diploma degree in physics from the University of Münster, Münster, Germany, in 1989 and the Dr. rer. nat. degree (Ph.D.) in physics from the University of Oldenburg, Oldenburg, Germany, in 1994. From 1989 to 2006, he was in different RD positions with Continental AG, Hanover, Germany, leaving as the Director of NVH Engineering (noise, vibration, harshness). Since 2006, he has been a full Professor with the Karlsruhe Institute of Technology (KIT), Karlsruhe, Germany. He is the Head with the KIT Institute of Vehicle System Technology, Karlsruhe and Scientific Spokesperson of the KIT Center Mobility Systems. His research interests include vehicle control, vehicle dynamics, vehicle NVH, vehicle suspension, tire dynamics, and tire road interaction as well as vehicle concepts, vehicle modeling, and identification methods.